


Future Virialized Structures

*An analysis of superstructures in
SDSS-DR7*



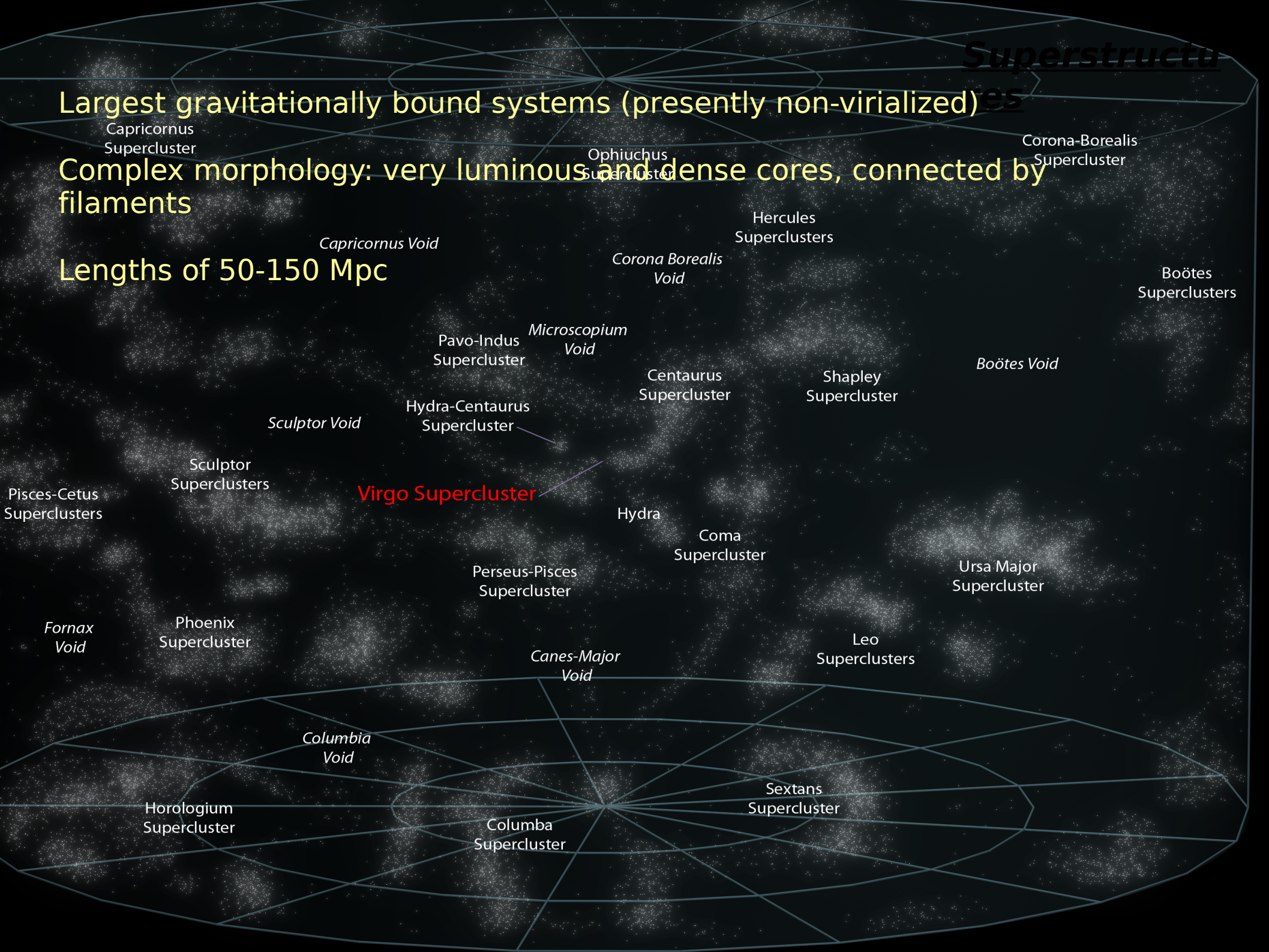
Heliana Luparello
Marcelo Lares
Diego García Lambas
Nelson Padilla

Superstructures

Largest gravitationally bound systems (presently non-virialized)

Complex morphology: very luminous and dense cores, connected by filaments

Lengths of 50-150 Mpc



Capricornus
Supercluster

Ophiuchus
Supercluster

Corona-Borealis
Supercluster

Complex morphology: very luminous and dense cores, connected by filaments

Capricornus Void

Hercules
Superclusters

Corona Borealis
Void

Boötes
Superclusters

Lengths of 50-150 Mpc

Microscopium
Void

Pavo-Indus
Supercluster

Centaurus
Supercluster

Shapley
Supercluster

Boötes Void

Sculptor Void

Hydra-Centaurus
Supercluster

Sculptor
Superclusters

Virgo Supercluster

Hydra

Coma
Supercluster

Ursa Major
Supercluster

Pisces-Cetus
Superclusters

Perseus-Pisces
Supercluster

Phoenix
Supercluster

Leo
Superclusters

Fornax
Void

Canes-Major
Void

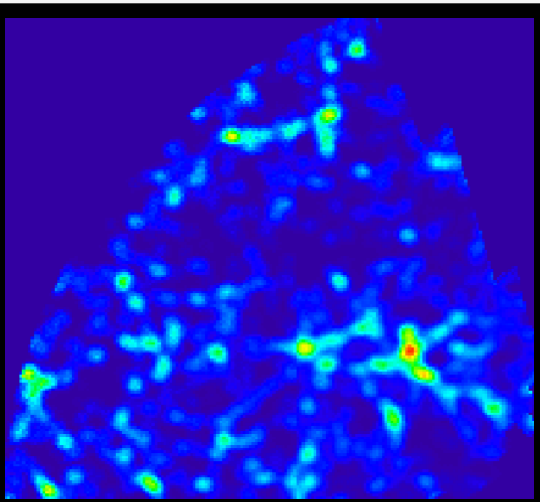
Columbia
Void

Sextans
Supercluster

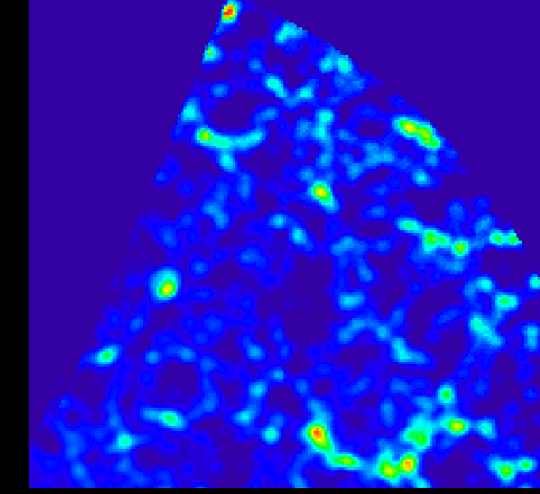
Horologium
Supercluster

Columba
Supercluster

Identification Process

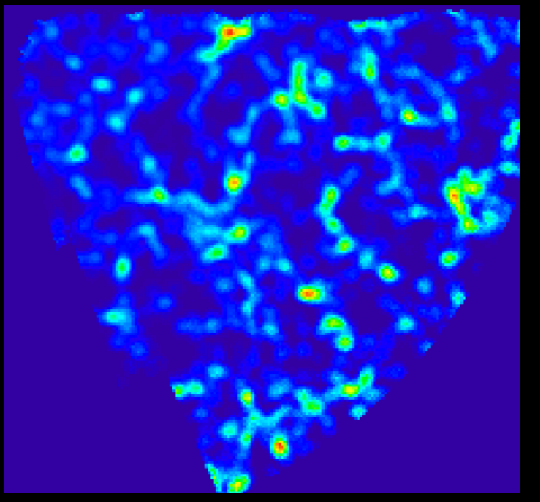


FoF algorithm on galaxy clusters (*Einasto et al., 1997*)
Percolation parameter?



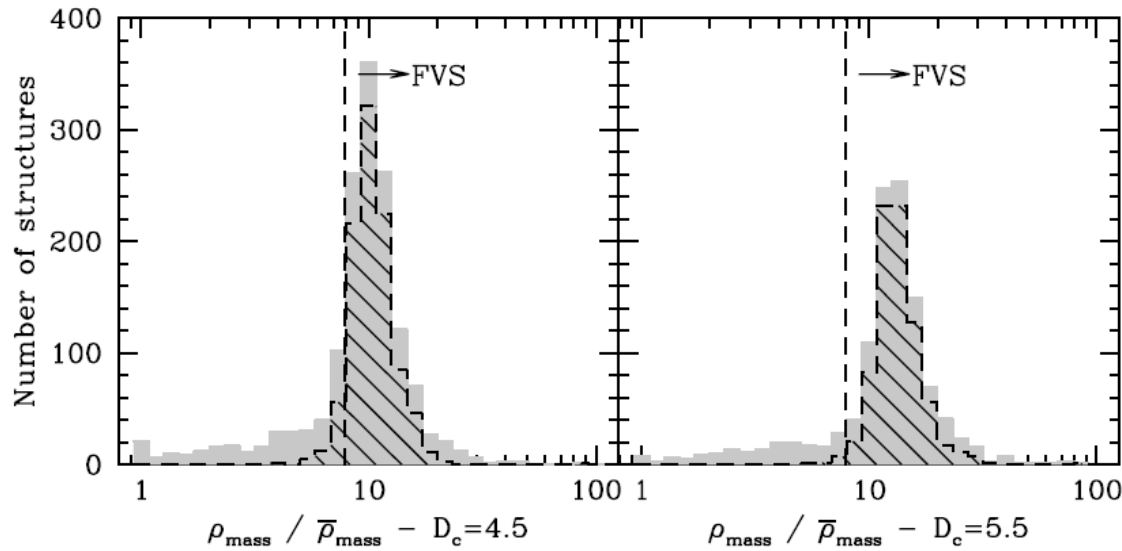
Luminosity-Density Maps (*Einasto et al., 2007*)

1. *smooth luminosity of galaxies --> Kernel*
2. *estimate luminosity density --> grid*
3. *connect overdense cells*



Luminosity overdensity threshold?

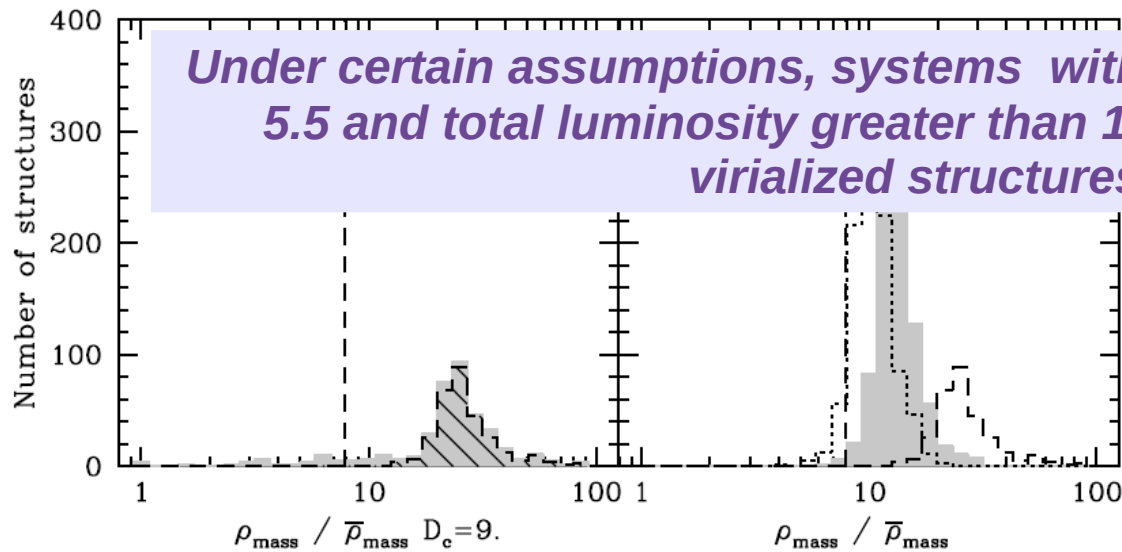
Threshold selection



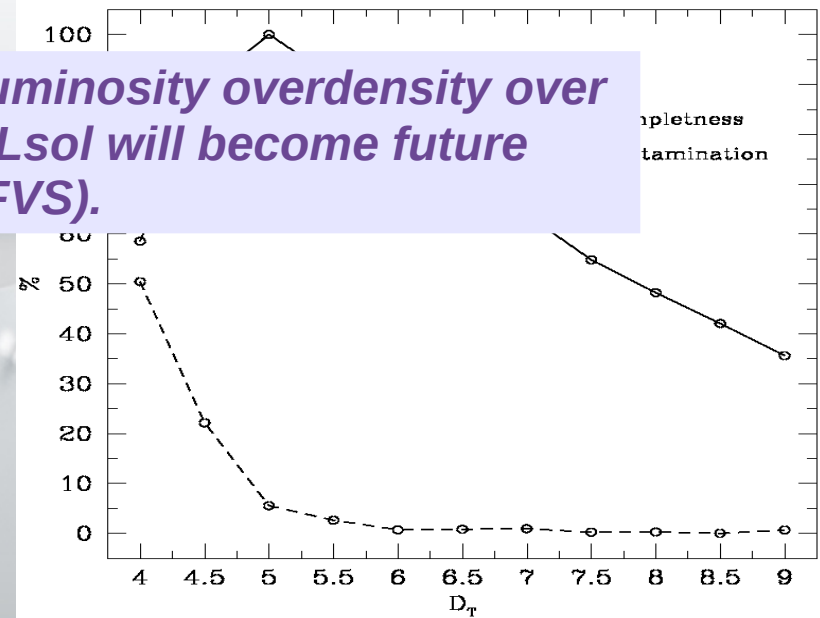
07)

remains gravitationally bound:

≥ 7.88



Under certain assumptions, systems with luminosity overdensity over 5.5 and total luminosity greater than $10^{12} L_{\text{sol}}$ will become future virialized structures (FVS).



An analysis of superstructures in SDSS-DR7

Future Virialized Structures on SDSS-DR7

Sample	z_{max}	$D_{max}[h^{-1} Mpc]$	M_r^{lum}	Volume [$10^7 (h^{-1} Mpc)^3$]	N_{gal}	$\bar{\rho}_{lum}[10^8 L_{\odot}/Mpc^3]$	F	Corrected $\bar{\rho}_{lum}[10^8 L_{\odot}/Mpc^3]$
S1	0.10	293.92	-20.05	1.85	94271	0.80	2.11	1.68
S2	0.12	351.34	-20.47	3.17	89513	0.58	2.98	1.73
S3	0.15	436.55	-21.00	6.01	62344	0.29	5.66	1.64
S2c	0.10	293.92	-20.47	1.85	51188	0.56	2.98	1.73
S3c	0.10	293.92	-21.00	1.85	17507	0.27	5.66	1.64
M_{Rsp}	0.12	351.34	-20.47	3.17	106604	0.75	2.98	2.23
						0.75	2.98	2.23

Sample	N_{FVS}	F_{vol}	F_{lum}	$glxs_{inFVS}$
S1	67	1.08%	10.85%	9707
S2	150	1.26%	13.54%	11394
S3	412	1.66%	20.61%	11682
M_{Rsp}	227	1.62%	18.87%	19265
M_{Zsp}	181	1.35%	15.14%	15368

Table 2. Main results obtained for the samples of identified FVS. For each sample, we show the number of future virialized structures N_{FVS} , the percentage of volume occupied by FVS F_{vol} , the percentage of luminosity of galaxies within FVS F_{lum} and the total number of galaxies within FVS $glxs_{inFVS}$.

de in the r-band is in the range $14.5 \leq r \leq 17.5$. The mean axes. The correction factor F (Eq. 6) and the resulting mean



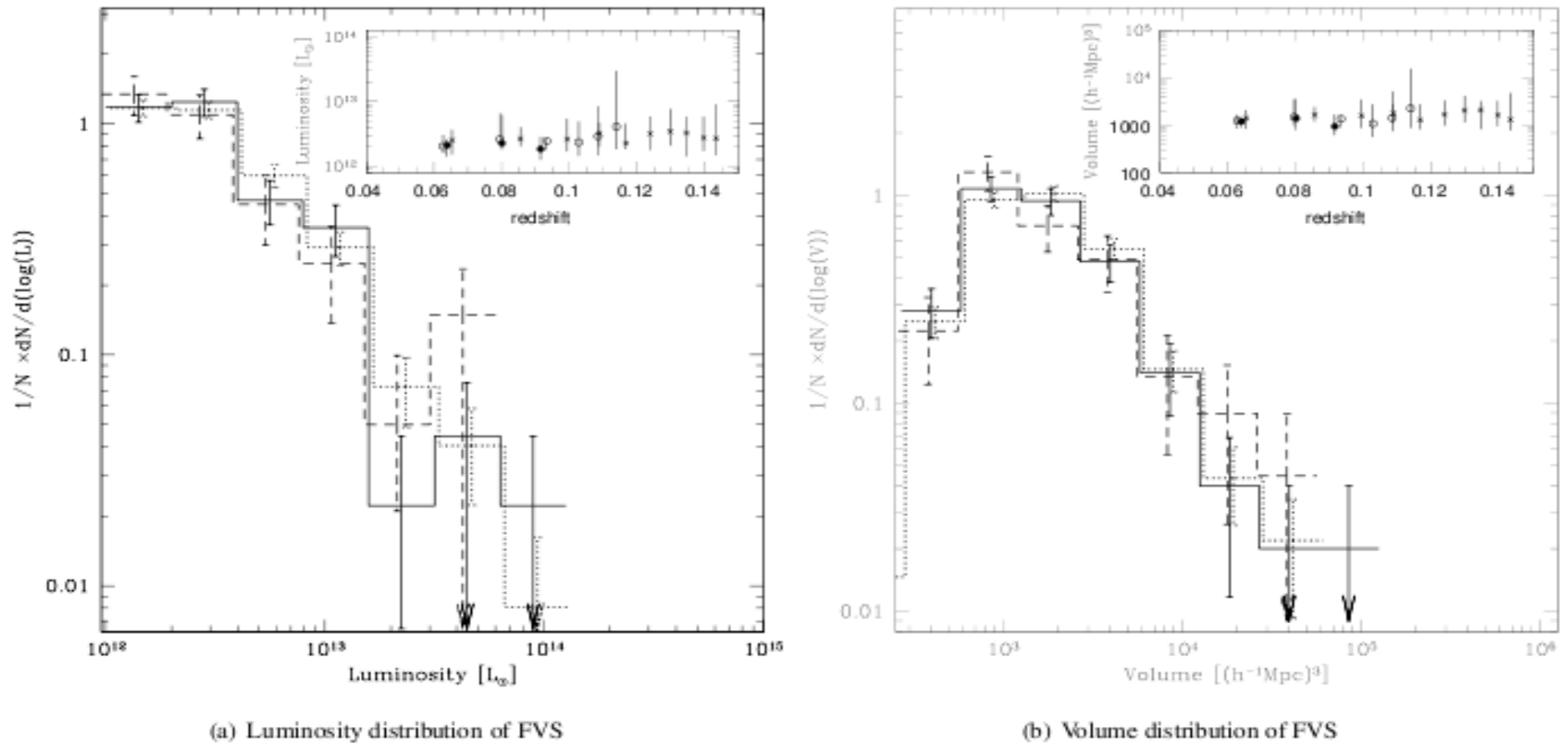


Figure 5. Luminosity and volume distributions of structures for samples S1 (dashed line), S2 (solid line) and S3 (dotted line). The insets show the average volume and luminosity as a function of the redshift, in redshift bins with equal numbers of superstructures, with filled circles, empty circles and crosses, respectively for samples S1, S2 and S3. Error bars on the histograms indicate Poisson uncertainty. In the inset box, the uncertainty bars correspond to the 25 per cent and 75 per cent percentiles.

Future Virialized Structures on SDSS-DR7

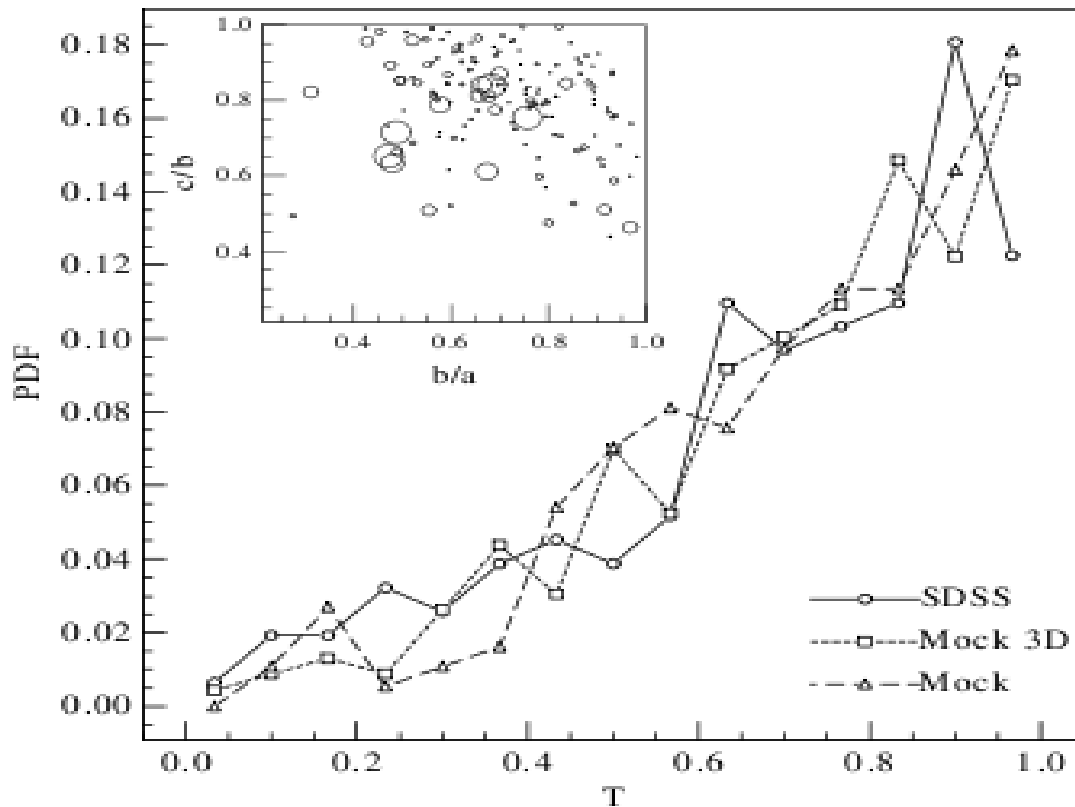


Figure 6. Probability density distribution estimates of the shape indicator parameter T (defined in section Section 4.1). The distributions correspond to FVS from the SDSS galaxy catalogue (solid line), the real-space mock catalogue (short dashed line) and the redshift-space mock catalogue (long dashed line). The inset shows a scatter-plot of the semi-axis ratios c/b and b/a that characterize the shapes of the FVS. The sizes of circles are proportional to the number of galaxies contained in each FVS.

$$T = (1 - (b/a)^2) / (1 - (c/a)^2)$$

$T \rightarrow 1$ indicates prolate structures

$T \rightarrow 0$ indicates oblate structures

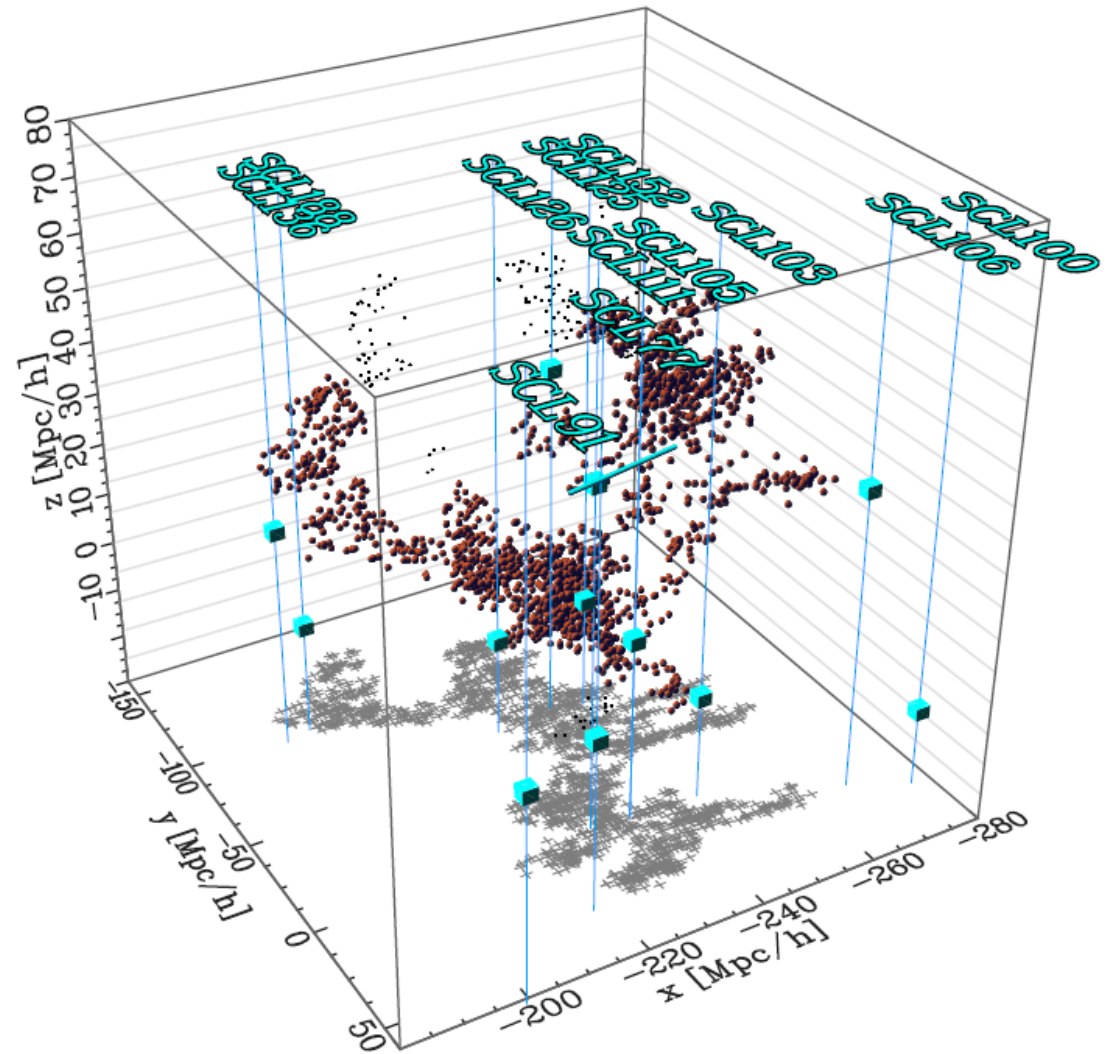
Redshift space vs. Real Space FVS

Lower number of FVS in redshift-space in comparison to real-space FVS.

20% of real-space structures are lost when analyzing redshift-space data.

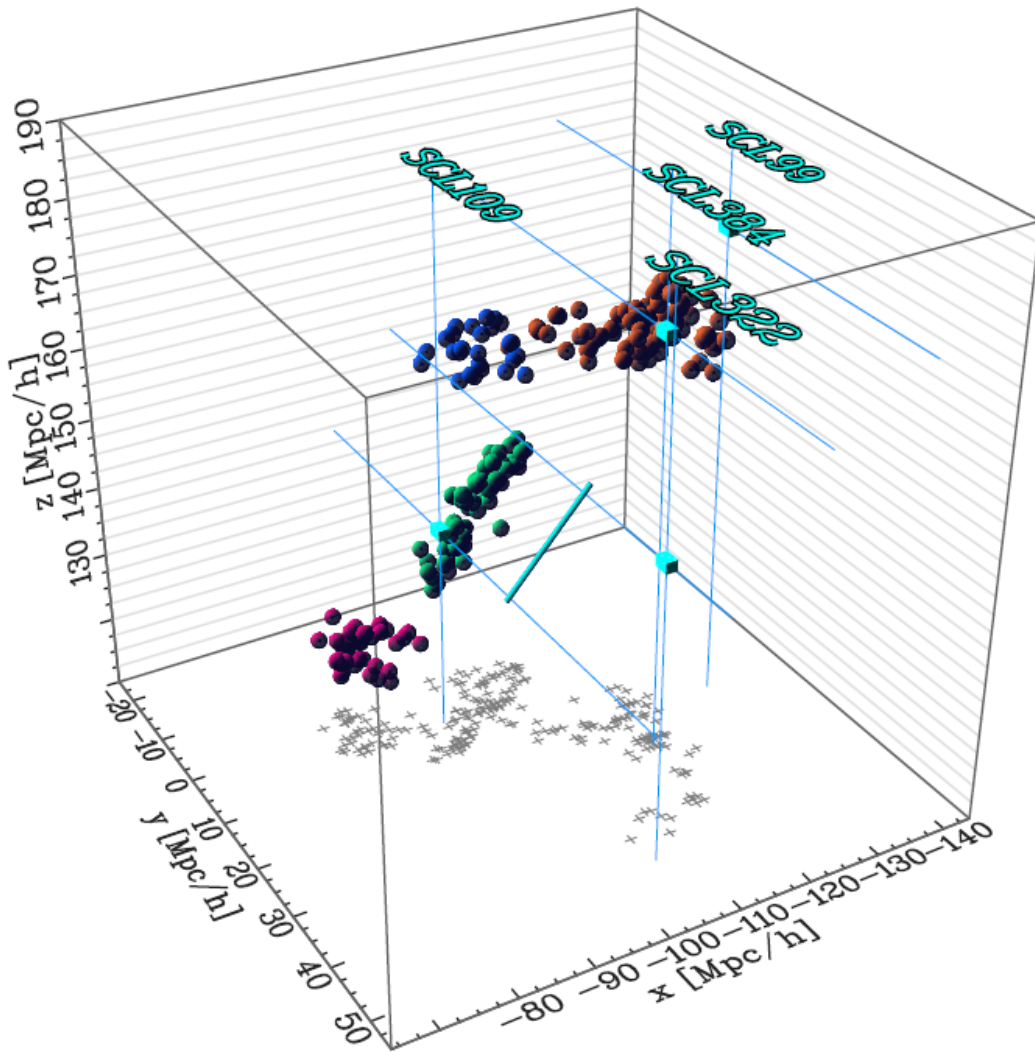
Only 2% of FVS identified in redshift-space are not real-space FVS.

3% of redshift-space FVS are associated with more than one FVS in real-space.



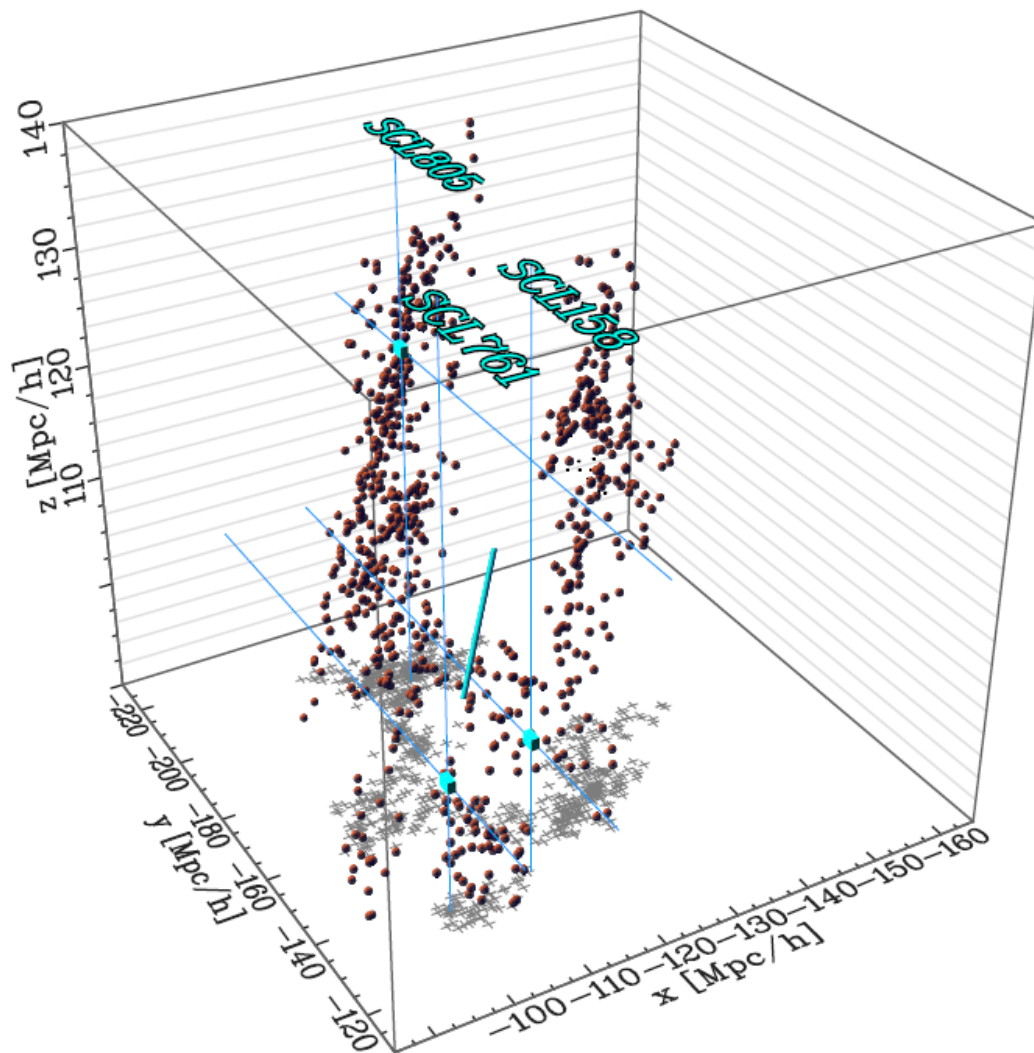
(a) Sloan Great Wall

... And Nostradamus

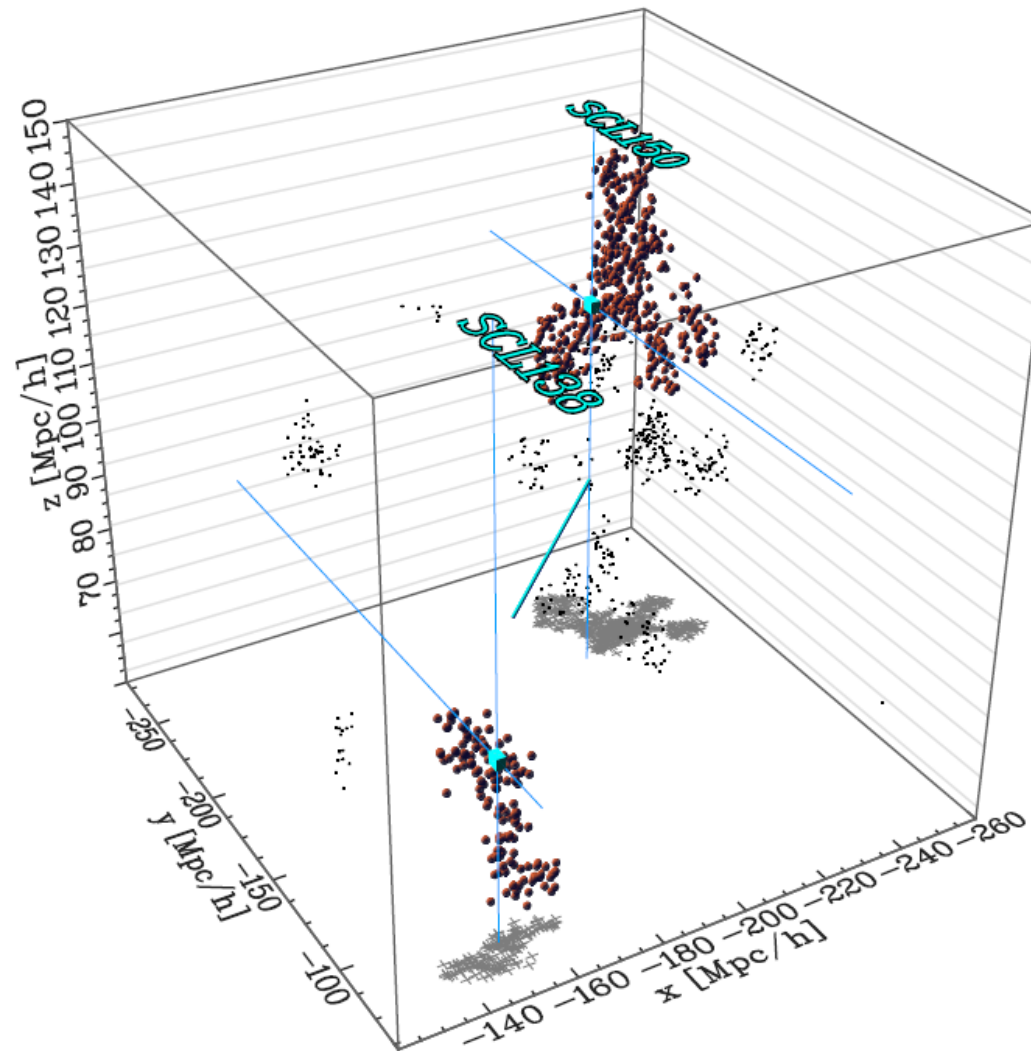


(b) Ursa Major supercluster

An analysis of superstructures in SDSS-DR7



(c) Corona Borealis supercluster



(d) Bootes supercluster